Hydrol. Earth Syst. Sci. Discuss., https://doi.org/10.5194/hess-2018-583
Manuscript under review for journal Hydrol. Earth Syst. Sci.
Discussion started: 13 December 2018

Hydrology and Earth System Sciences
Open Access
Discussions

# Numerical study on the response of the largest lake in China to climate change

Dongsheng Su[1, 2], Xiuqing Hu[3], Lijuan Wen[1], Lin Zhao[1], Zhaoguo Li[1], Juan Du[1, 2], Georgiy Kirillin[4]

[1]Key Laboratory of Land Surface Process and Climate Change in Cold and Arid Region, Northwest Institute of Eco-Environment and Resources, Chinese Academy of Sciences, Lanzhou, 730000, China
[2]University of Chinese Academy of Science, Beijing 100049, China
[3]National Satellite Meteorological Centre, Beijing 100081, China
[4]Department of Ecohydrology, Leibniz-Institute of Freshwater Ecology and Inland Fisheries (IGB), 12587 Berlin, Germany

*Correspondence to*: Lijuan Wen (wlj@lzb.ac.cn)

**Abstract.** Lakes are sensitive indicators of climate change. There are thousands of lakes on the Tibetan Plateau (TP), more than 1200 of them having an area larger than 1 km$^2$, but few observation data of lakes are available. Therefore, the thermal condition of the plateau lakes under the background of climate warming remain poorly understood. In this study, the China Meteorological Forcing Dataset developed by Institute of Tibetan Plateau Research, Chinese Academy of Sciences (ITPCAS), MODIS Land Surface Temperature (LST) data and buoy observation data were used to reveal the response of thermal conditions of Qinghai Lake to the recent climate change and to analyze the applicability of Freshwater Lake Model (FLake) to Qinghai Lake. Despite some deviations caused by model simplifications and uncertain forcing data, FLake demonstrated a good ability in capturing the seasonal variations of the lake surface temperature and the internal thermal structure of Qinghai Lake. The simulated lake surface temperature demonstrated a positive trend from 1979 to 2012, positively correlated with the air temperature and the downward longwave radiation, while negatively correlated with the wind speed and with the solar radiation but failing to pass the significance test. The simulated internal thermodynamic structure revealed that, if the impact of salinity is not considered, the Qinghai Lake is a dimictic lake with two overturn periods occurring in late spring and late autumn respectively. The surface and mean water temperatures significantly increased from 1979 to 2012, while the bottom temperatures showed no significant trend, even decreasing slightly from 1989 to 2012. The warming was the strongest in winter for both LST and air temperature. With the warming of the climate, the later ice-on and earlier ice break-up were simulated, having a strong effect on lake-air temperature differences in January and May.

## 1 Introduction

The Tibetan Plateau (TP) is the highest plateau in the world, known as the Earth's "third pole" (Qiu, 2008), and exerts a significant influence on regional and global atmospheric circulation through its dynamic and thermodynamic effects (Yanai et al., 1992; Duan et al., 2005). The TP is also one of the most sensitive regions to climate change: the surface air temperature increase over the TP due to global warming is stronger than in other regions (Guo et al., 2012; Duan et al., 2015). Apart from warming, an increase of air humidity and precipitation, and a decrease of short-wave radiation and wind speeds were reported for the central TP since the beginning of the 1980s (Liao et al., 2013; Yang et al., 2014). Thousands of lakes are scattered across the TP, accounting for 39.2% of the entire number and for 51.4% of the entire area of Chinese lakes (Ma et al., 2011). Lakes are an inherit components of the hydrological system of TP, named "the world water tower" (Xu et al., 2008), contributing essentially to the water cycle between atmosphere, glaciers and the major Asian rivers. Due to the significant increase in precipitation and melting of glaciers caused by climate change, the total area of lakes tended to expand significantly on the TP since the late 1990s (Lei et al., 2014; Liao et al., 2013). Large lake areas significantly influence the local and regional weather and climate, mainly because of their differences in albedo, heat capacity, roughness, and energy exchange compared to the land surfaces around (Bonan et al.,1995; Eerola et al., 2010).

In their turn, lakes are very sensitive to climate, and their physical, chemical and biological properties respond rapidly to a climate-related change (Adrian et al., 2009; Williamson et al.,2009). The surface water warming rates of lakes are mainly driven by the increasing air temperature (Adrian et al., 2009; Schmid et al., 2014), depending on combinations of climate and local characteristics, associated with interactions among different climatic factors. In most of the lakes, surface water is warming around the globe, whereas some lakes are cooling or do not reveal any significant temperature trends (O'Reilly et al.,2015). Global warming also has an impact on the vertical thermal structure of lakes and cause mixing regimes shifting (Livingstone, 2003, 2008; Boehrer and Schultze, 2008). Surface warming increases the summer vertical stability and prevents the heat transfer to the bottom of the lake, so that a counter-trend of cooling may occur at the bottom (Kirillin et al., 2010). Warming also may result in drastic shifts in the date of lake ice break-up and freeze-up (Weyhenmeyer et al., 2004), which can significantly influence the seasonal thermal and energy regimes of the lakes (Rouse et al., 2003). The ice-on and ice break-up dates on lakes and rivers demonstrate a long-term trend on later freezing and earlier break-up around the Northern Hemisphere, as a response to corresponds to the increase in air temperature of about 1.2 ° per 100 years (Magnuson et al., 2000).

Same as globally, both warming and cooling trends occurred in the lakes on TP (Zhang et al., 2014a). Due to the high elevation and low atmospheric density over the TP, the surface received solar radiation input is larger than in lowland areas that results in large diurnal amplitudes of surface temperature (Gao et al., 1981; Ma et al., 2009). During the last decades, a negative trend in the solar radiation flux is observed over the TP, which can be ascribed to the increase of the air humidity (Shen et al., 2015). As a result, lakes are predicted to experience a cooling trend despite a significant increase of the air temperature over the plateau (Kirillin et al., 2017) that demonstrates decoupling of air and land response to the global change and suggests a non-linear response of the entire hydrological system.

Only few observation data are available for the Tibetan lakes due to the harsh environment on TP; therefore, the lake thermal conditions and their response to climate change are far from being well understood. Hence, numerical simulation appears to be a most efficient approach in lake investigation on TP, provided that the numerical model is well-calibrated and reliable information on the atmospheric forcing is available.

In this paper, we model brackish endorheic Qinghai Lake — the largest lake on TP and in China— to reveal the major features of the TP lake response to climate change. We used the lake model FLake (Mironov., 2008), which is a highly parameterized one-dimensional lake model aimed primarily at lake representation in land schemes of regional climate models. FLake was numerously tested before for different lakes worldwide (Kirillin, 2010; Bernhardt et al., 2012; Stepanenko et al., 2013; Thiery et al., 2014), including freshwater lakes of the TP (Kirillin et al., 2017). The strength of FLake is its high computational efficiency combined with a realistic representation of the major physics, which made the model to a basic tool for lake representation in the land schemes on the global scale (e.g., Dutra et al., 2010; Salgado and Le Moigne, 2010; Rooney and Bornemann, 2013; Mallard et al., 2014). However, FLake is originally a freshwater lake model taking no account for salinity effects on mixing and heat exchange with the atmosphere. While saline and brackish lakes represent only a small part of inland water bodies, they may have an appreciable effect on the land-atmosphere interaction in arid regions. Therefore, in addition to quantifying the recent climate change effects on the thermal regime of China's largest lake, the second aim of the study was to test the FLake performance on brackish lakes. Here, we intentionally applied the freshwater lake model to a brackish lake in order to (i) evaluate the ability of the lake model FLake to simulate the main thermodynamic features of the lake in high-altitude conditions and (ii) validate the performance of freshwater lake model for a brackish lake.

## 2 The study area, Data, and Methodology

### 2.1 Study area

Qinghai Lake (36°32′-37°15′ N, 99°36′-100°47′ E, 3194 m a.s.l.) is the biggest lake in China with a surface area of 4497 km$^2$ (in 2017) and a catchment area of 29660 km$^2$. The maximum length and width of the lake are approximately 106 and 67 km respectively. It is an endorheic, brackish lake (salinity 12.5 g·L$^{-1}$, pH 9.3) (Deng et al., 2010) located on the northeast margin of the TP (Fig. 1). The mean and maximum depths of the lake are 21 and 32.8 m, respectively. The lake usually freezes up in December/January and the ice breaks up in early April. The average annual lake water temperature is 5.4 °C, with a maximum monthly temperature of 17.2 °C (August) and a minimum of -2.0 °C (January) (Li et al., 2016). The average annual air temperature (1959-2015) at the lake is 1.9 °C. The mean annual precipitation in 1959-2015 was about 340 mm (Ding et al., 2018) with more than 65 % occurring in summer. Annual evaporation from the lake surface was 924 mm, surface runoff water inflow and groundwater inflow were 348 and 138 mm respectively (Li et al., 2007).

Qinghai Lake is sensitive to climate change. The annual temperature of the Qinghai lake basin increased remarkably by about 0.3 °C per decade from 1961 to 2012 and the water level decreased at the average rate of 7.6 cm per year from 1961 to 2004 (Cui et al., 2016). According to the data from Gangcha station (the nearest meteorological station approximately 13 km north to Qinghai Lake), precipitation continuously increased in 1970-2015 by 15.603 mm per decade, especially after 2005; coupled with the melting of Qilian Mountain glaciers that increased the runoff to the lake, and the decreasing evaporation by 1.343 mm per year (Gangcha station) during 1970-2003 (Tang et al., 2018). Since 2004, the Qinghai lake stopped shrinking and began to expand, lake level increased at a rate of 14 cm per year during the period 2004-2012; and the regional climate gradually turned to the direction of "warm and humid" (Dong and Song, 2011; Zhang et al., 2011, 2014b; Cui et al., 2016).

## 2.2 Data

### 2.2.1 Buoy observation data

The observation data were obtained from the Qinghai Lake hydrological automatic meteorological observation buoy (36.68° N, 100.50° E). The recorded parameters included air temperature, wind direction, wind speed, pressure, relative humidity, surface water temperature at 0.7 m below the surface, dew point temperature and water salinity. The observation period was confined to the summer and autumn open water periods from 2001 to 2005 (Fig. 2), with an observation interval of 3 hours.

### 2.2.2 MODIS Lake Surface Temperature

The gaps in the long-term buoy observations were caused by harsh environmental conditions and the long ice cover period. Therefore, the 8-day MODIS LST product (MOD11C2), which covers 2001-2012, was additionally used to evaluate the long-term simulated results. This product offers 8-days combined radiative surface temperature approximately at 10:30 and 22:30 local time, which is the satellite transit time, with a resolution of 5 km (Wan et al., 2004). Here we used a single point of MODIS LST closest to the buoy location in order to be comparable with the buoy observed data. The MODIS data comparison against the buoy data found them generally consistent, except rare abnormal values influenced probably by cloud cover (Langer et al., 2010). MODIS LST was generally lower than buoy observations, with the mean for the five years under consideration about -0.36 °C (Fig. 2). The bias might be attributed to the cool skin phenomenon making the radiation temperature to be typically lower than the bulk temperatures (Robinson et al., 1984; Donlon et al., 2002; Minnett et al., 2003; Leppäranta and Lewis, 2007).

### 2.2.3 ITPCAS Forcing Data

The China regional surface meteorological feature dataset (He, 2010) developed by Data Assimilation and Modeling Center for Tibetan Multispheres, the Institute of Tibetan Plateau Research, Chinese Academy of Sciences (hereafter ITPCAS) was used as atmospheric forcing data for the FLake model. The version used here covers the period of 1979-2012. It was produced by merging a variety of data sources, including Princeton meteorological forcing data, Global Land Data Assimilation System (GLDAS) data, The Global Energy and Water Cycle Experiment-Surface Radiation Budget (GEWEX-SRB) shortwave radiation dataset, Tropical Rainfall Measuring Mission (TRMM) satellite precipitation analysis data and China Meteorological Administration (CMA) station data. The ITPCAS forcing data set includes air temperature and specific humidity at 2 m height above the ground, wind speed at 10 m height, surface pressure, precipitation, and downward shortwave and longwave radiations at a spatial resolution of 0.1° and a temporal resolution of 3 hours (He and Yang, 2011). The downward longwave radiation was calculated by the model of Crawford and Duchon's (1999) as a function of air temperature, pressure, specific humidity, and downward shortwave radiation. ITPCAS forcing incorporates CMA station data; therefore, it is more accurate in this region of China compared with other data sets and is generally preferable for modeling studies in China (Chen et al., 2011; Guo and Wang, 2013; Liu and Xie, 2013).

### 2.3 Lake model

The FLake model (Mironov, 2008) is used to simulate the vertical temperature profile and the energy budget of the different layers of the lake on the time scales from several hours to many years. The model divides the lake water body vertically into two layers, the upper layer being the mixed layer with uniform temperature. Beneath the mixed layer, the temperature profile is parameterized using the concept of self-similarity (Kitaigorodskii and Mirokolskii, 1970), which means that the characteristic shape of the temperature profile is conserved irrespective of the depth of this layer. Additionally, FLake includes the representation of the thermal structure of the ice layer, snow layer and the thermally active upper layer of bottom sediments, all using the self-similarity concept. This simple two-layer parameterization of the water column provides FLake with computational efficiency, while preserves the essential physics. The snow module of FLake has not been comprehensively tested so far. The mixed layer depth is computed by using different evolution equations for cases of convective mixing and wind mixing in stable or neutral stratification. Compared with other lake models, it is relatively easy to adjust FLake to a specific application due to a small number of lake parameters to be specified, the major ones being the lake depth and the optical characteristics of the lake water. Here we set the lake depth to be the mean depth of Qinghai Lake (21 m). The simulation started at the beginning of the year 1979, when the lake surface began to freeze, so that the initial water temperatures were set to 273.15 K for the mixed layer and 277.15 K for the lake bottom. The forcing data in 1979 were used to drive the Flake model 10 iterations for spin-up. Then the actual modeling period started from 1979 and ended in 2012. The simulation duration was 34 years with the simulation step of 3 hours.

## 3 Results

### 3.1 Simulated lake temperatures

Comparison of the simulated lake surface temperatures against MODIS LST (Fig. 3) demonstrated that the FLake model can nicely simulate the seasonal variations of the lake surface temperature, the correlation amounted at 0.94. The simulated temperature was however generally higher than the MODIS LST, with a positive bias of 1.71 °C and an RMSE value of 3.87 °C for annual mean, except in springtime, where the simulated LST had a negative bias of -1.74 °C compared to MODIS LST.

In order to evaluate the effect of the forcing data deviation on the simulation results, we applied a correction to the ITPCAS forcing data. Since the buoy observations are mainly available from June to October, only forcing data for this period of the year was correct. The air temperature was adjusted with the linear relationship ($y = 0.76x + 3.27$, x for ITPCAS and y for buoy observations) and the wind speed was corrected by adding a constant bias of 1.19 $m \cdot s^{-1}$ between the mean buoy observation and the mean ITPCAS data. After the correction, the bias and root-mean-square error (RMSE) between simulated LST and

MODIS LST both reduced (from 1.71 °C and 3.87 °C to 1.12 °C and 3.49 °C respectively), especially for the bias in summer (2.95 °C to 2.48 °C) and autumn (3.55 °C to 2.72 °C). The remaining bias may be attributed to the cool skin effect in the LST sensed by MODIS, so that performance of FLake for bulk surface temperatures may be even better.

The effect of salinity on the lake mixing was not accounted for by the FLake model, assuming purely thermal stratification. The modeled seasonal stratification of Qinghai Lake corresponded to that of a dimictic lake (Fig. 4) with typical features of this type of mixing regime (Kirillin and Shatwell, 2016). Winter and summer stratified periods are divided by two short periods of full vertical mixing (overturns) in late spring and late autumn. During the overturn period, dimictic lakes are supposed to be fully mixed to the bottom. From the simulation, we found that the spring overturn of Qinghai Lake, occurring around May, lasted for 2-3 weeks and the depth of mixed-layer reached the bottom of the lake in most but not all simulation years. The autumn overturn appeared around November-December, lasted approximately for a month, and the mixed-layer reached the bottom of the lake in all simulated years. In the summer stratified period, the mixing process was mainly caused by the wind forcing and the stratification instability due to diurnal temperature variations, and the depth of the mixed layer reached 10-15 m, gradually increasing with time.

When compared to MODIS LST, the modeled LST were lower in the spring and higher in other seasons, especially in summer and autumn; the deviations were stronger in nighttime than during daytime. Qualitatively, the model simulated the variations of the LST and its typical magnitudes well, as well as produced a reasonable vertical thermal structure.

### 3.2 Response of lake thermal conditions to the long-term trends in external forcing

According to the ITPCAS data from 1979-2012, the air temperature and long-wave radiation had positive trends of 0.58 °C ($p<0.01$) and 3.22 $W \cdot m^{-2}$ ($p<0.01$) per decade respectively, while the wind speed and short-wave radiation had a negative trend of -0.11 $m \cdot s^{-1}$ ($p>0.05$) and -2.41 $W \cdot m^{-2}$ ($p<0.05$) per decade respectively. These values are consistent with other reports on climate change over the TP: The air temperature at different weather stations on TP is rising by an average of 0.09 °C to 0.74 °C per decade from 1961 to 2007 (Guo and Wang, 2012), while, the wind speed and short-wave radiation is decreasing (Yang et al., 2014).

From 1979 to 2012, the simulated LST, mixed-layer temperature, and the lake mean temperature was increasing at 0.66 °C, 0.29 °C and 0.27 °C per decade respectively ($p<0.01$ for all three trends); the bottom temperature revealed a slower trend at 0.14 $°C \cdot decade^{-1}$ ($p>0.05$, failing to pass the significance test) (Fig. 5). For the first decade from 1979 to 1989, all temperatures demonstrated a stronger warming trend, especially for the surface layer (1.2 $°C \cdot decade^{-1}$). Later on, the trend slowed down to 0.52 $°C \cdot decade^{-1}$ for the surface temperature and 0.19 $°C \cdot decade^{-1}$ for both mixed-layer and mean water column during the rest of years. The bottom water temperature even demonstrated a slightly decreasing trend of -0.03 $°C \cdot decade^{-1}$ ($p>0.05$, failing to pass the significance test).

Due to the importance of the lake surface as an interface of heat and mass exchange between the lake and air, the trend in the LST was investigated in the relationship to the main atmospheric characteristics (Fig. 6). The trend of LST simulated by FLake was consistent with rising air temperature (0.58 °C per decade) but with a higher rate of 0.66 °C per decade, having a positive correlation coefficient of 0.75 ($p<0.01$) with air temperature. A negative correlation coefficient of -0.33 ($p >0.05$, failing to pass the 0.05 significance test) was found between the simulated LST and the wind speed. The downward short-wave radiation had a negative correlation coefficient of -0.27 ($p>0.05$, failing to pass the 0.05 significance test) to the LST. The LST and the downward long-wave radiation were positively correlated (coefficient of 0.76, $p<0.01$).

### 3.3 Lake ice cover

The variations of break-up and freeze-up dates are sensitive to the meteorological conditions, in the first place, air temperature, solar radiation, and wind (Duguay et al.,2006; Latifovic et al., 2007; Ye et al., 2011; Kirillin et al., 2012; Yao et al., 2016). The simulated maximum ice thickness demonstrated a negative correlation of -0.58 ($p<0.01$) to the mean air temperature anomaly from January to April at Qinghai Lake. With the increase of air temperature, the maximum ice thickness of Qinghai Lake revealed a decreasing trend of 0.07 $m\cdot decade^{-1}$ ($p<0.01$) (Fig. 7a). Simulated ice cover of Qinghai Lake started in the late December to early January and ended in late April to early May. The correlation of -0.61 was found between the break-up date and mean air temperature anomaly for April-May ($p<0.01$) (Fig. 7b), while a 0.64 ($p<0.01$) correlation was found between freeze-up date and mean temperature anomaly for November-December (Fig. 7c). With the increasing trend in the air temperature and LST, the break-up date advanced about 4 days earlier every decade and the freeze-up date delayed also about 4 days later every decade, resulting in shortening of the ice cover period at about 8 days per decade (Fig. 7d).

### 3.4 Interannual variation of energy balance

Lake mean temperature is the indicator of the heat storage by the lake water body, whose changes are mainly driven by the heat exchange at the lake surface, the latter which is composed of net (shortwave and longwave) radiation budget, sensible heat flux (SH) and latent heat flux (LH). Quantification of the energy balance at the lake surface is necessary for understanding the mechanisms of the lake response to climate change. The heat transfer from precipitation, runoff and the bottom sediments of the lake are ignored here due to their small magnitudes and observational difficulties.

According to ITPCAS data, the solar radiation flux over Qinghai Lake is decreasing at -2.41 $W\cdot m^{-2}$ per decade ($p<0.05$) (not shown), while simulation results produce a positive trend of 2.35 $W\cdot m^{-2}$ ($p <0.05$) per decade in the net short-wave radiation income to the lake (Fig. 8a). This is caused apparently by shortening of the ice-covered period from 127 days (1979) to 93 days (2012) that reduced the lake surface albedo from the ice values (between 0.1 and 0.6) to the open water albedo (~ 0.07), increasing by this the net annual solar radiation absorption by the lake. The net long-wave radiation reduced at -1.86 $W\cdot m^{-2}$ per decade ($p<0.05$) (Fig. 8b). At the same time, the downward longwave radiation increased at 3.22 $W\cdot m^{-2}$ per decade ($p<0.01$) (not shown), i.e. the net long-wave radiation trend was caused by the increased upward longwave radiation (5.08 $W\cdot m^{-2}$ per decade, $p<0.01$) due to the rising LST during the open water period and shortening of the ice cover duration.

From 1979 to 2012, SH at Qinghai lake decreased at -0.19 $W\cdot m^{-2}$ per decade ($p>0.05$, failing to pass the 0.05 significance test) (Fig. 8c), while LH become stronger at 0.99 $W\cdot m^{-2}$ per decade ($p>0.05$, failing to pass the 0.05 significance test) (Fig. 8d). Hence, the additional heat gained due to the net radiation increase was mainly balanced by the increased LH due to evaporation.

Hydrol. Earth Syst. Sci. Discuss., https://doi.org/10.5194/hess-2018-583
Manuscript under review for journal Hydrol. Earth Syst. Sci.
Discussion started: 13 December 2018

### 3.5 The lake-air temperature difference and the radiation flux

The lake-air temperature difference is one of the major factors determining the surface heat exchange. The strong seasonal variation of the surface-air temperature differences is driven by the different thermal properties of the lake and the surrounding land surface (Haginoya et al., 2009; Desai et al., 2009). Averaged from 1979 to 2012, the 5-day moving average air temperature is higher than LST during the ice duration period (Fig. 9a), with the minimum lake-air temperature differences as low as -7.27 °C (Fig. 9b). After the ice-off between late-April to mid-May, LST increased rapidly, particularly under the heating by the intense solar radiation (maximum 285.4 $W \cdot m^{-2}$ for 5-day average), characteristic for high-altitude conditions on TP (Fig. 9c), and exceeded the air temperature in June, reaching the maximum of 18.9 °C in August (Fig. 9a). LST was generally higher than air temperature from June to January of the next year, which roughly coincided with the end of the open-water period. The mean lake-air temperature difference (5-day moving average) became positive in June and kept increasing to a maximum of 13.56 °C in December just about 10-20 days before the ice cover formation (Fig. 9b). Owing to the large heat capacity of the lake, a clear phase lag existed between LST and air temperature. The time difference between the seasonal temperature maximums of the LST and the air temperature was about 20 days, and the time difference between both values dropping to the freezing temperature of water of 0 °C was about 2 months.

Both air temperature and LST had an increasing trend all year round, with stronger warming in winter than in summer (Fig. 9a). Although the downward longwave radiation increased in summer and autumn (average of 0.33 $W \cdot m^2 \cdot a^{-1}$, maximum of 0.47 $W \cdot m^2 \cdot a^{-1}$ in September) (Fig. 9d), the LST increased slower than the air temperature resulting in a slight reduction of lake-air temperature difference (average of -0.013 $°C \cdot a^{-1}$, maximum of -0.04 $°C \cdot a^{-1}$ in November) (Fig. 9b). This behavior can be attributed to the apparent decrease of the shortwave solar radiation in summer (average of -0.59 $W \cdot m^2 \cdot a^{-1}$), which reduced the summer net shortwave radiation input to the lake (average of 0.33 $W \cdot m^2 \cdot a^{-1}$, Fig. 9c, e). In turn, the increased upward longwave radiation in summer and autumn (average of ~ 0.17 $W \cdot m^2 \cdot a^{-1}$) (not shown) partially damped the effect of downward longwave radiation increase (average of 0.33 $W \cdot m^2 \cdot a^{-1}$), which lead to a decrease of the net longwave radiation from the lake to air (average of ~ 0.16 $W \cdot m^2 \cdot a^{-1}$) (Fig. 9f).

In contrast to the depressed trend of LST increase during the ice-free period, the monthly mean LST in early winter and late spring increased more rapidly than the air temperatures, with two apparent peaks of 0.13 $°C \cdot a^{-1}$ and 0.07 $°C \cdot a^{-1}$ in January and May, respectively (Fig. 9a, b). The significant increase of LST in these periods may be related to the shift of the ice-on and break-up dates (gray areas in Fig. 9), as well as to the slight increase of solar radiation in December and April. The same seasonal pattern is reflected in the variations of the radiation balance (Fig. 9e, f): During the open-water period, the net shortwave (longwave) radiation has a consistent trend with downward shortwave (longwave) radiation, while in the freezing period (the gray area around December-January in Fig. 9) and the thawing period (the gray area around April-May in Fig. 9) both net and downward shortwave (longwave) radiation fluxes had opposite trends. The net shortwave radiation increased obviously in these two periods (average of 0.79 $W \cdot m^2 \cdot a^{-1}$ and 1.6 $W \cdot m^2 \cdot a^{-1}$ respectively) while the downward shortwave radiation was not (average of -0.05 $W \cdot m^2 \cdot a^{-1}$ and -0.13 $W \cdot m^2 \cdot a^{-1}$ respectively) (Fig. 9c, e). The same is true for the net longwave radiation that decreased obviously in these two periods (-1.06 W·m$^2$·a$^{-1}$ and -0.61 W·m$^2$·a$^{-1}$ respectively) although the downward longwave radiation has an increasing trend in each period (0.34 W·m$^2$·a$^{-1}$ and 0.16 W·m$^2$·a$^{-1}$) (Fig. 9d, f).

### 3.6 Heat budget during ice-on and ice-off

Since the dates of the lake ice break-up and freeze-up strongly affect the seasonal energy budget of the lake (Rouse et al.,2003; Jakkila et al., 2009), the heat budget and its long-term trends were considered in more details.

During the thawing period (the gray area around April-May in Fig. 10, same as in Fig. 9), the solar radiation was the strongest (average of 277 W·m$^{-2}$, Fig. 9c), on the background of appreciable downward longwave radiation (average of 257 W·m$^{-2}$, Fig. 9d). An earlier break-up date significantly reduced the albedo of the lake (from ice ~ 0.6 to water ~ 0.07), which increased the net shortwave radiation flux into the lake (Fig. 9e), same for the net radiation in April and May (average of 1.08 and 0.91 W·m$^{-2}$·a$^{-1}$ respectively, Fig. 10c). Concurrently, the small lake-air temperature differences also ensured small SH and LH (average of -2.1 and 8.9 W·m$^{-2}$ respectively, Fig. 10a, b), which means the heat release from the lake surface (the compound of net longwave radiation, SH, and LH) is low (Fig. 10d). As a consequence, the net energy flux (Q) gained by the lake in this period (average of ~ 69.6 W·m$^{-2}$) increased due to earlier ice breakup at 0.9 W·m$^{-2}$·a$^{-1}$ or at ~ 13% per decade (Fig. 10e).

In contrast, the freezing period (the gray area around December-January in Fig. 10) was characterized by the weakest levels of both short-wave and downward longwave radiation (average of ~123 W·m$^{-2}$ and ~167 W·m$^{-2}$ respectively, Fig. 9c, d). The upward longwave radiation (not shown) before freeze-up was ~ 1.5 times larger than downward longwave radiation, with a minimum of net radiation in December of -47.6 W·m$^{-2}$ (Fig. 10c). Also, unlike the ice-off, the values of upward SH and LH (average of 19 and 25 W·m$^{-2}$ respectively) both cannot be ignored because of a large lake-air temperature difference during the ice cover formation. Hence, a later ice-on leads to intense cooling by the upward longwave radiation, SH and LH at the lake surface not arrested by the ice cover (Fig. 10 a, b, c, d). The additional heat absorbed by the lake caused by earlier break-up in previous seasons released before freeze-up partly contributed to the delay of the freeze-up date of Qinghai Lake.

## 4 Discussions and Conclusions

### 4.1 Model performance

The validation results indicate that FLake performed well for the extreme climatic conditions of TP; it reproduced well the observed seasonal variation of LST and reasonably simulated the thermal structure of the mixed layer and the thermocline. Although there was an underestimation to the lake surface temperature in spring and an overestimation of it in rest of the seasons, FLake can be considered a useful tool to study the impact of the climate change to lakes on TP.

The ITPCAS forcing data incorporating observations from land weather stations, produced a constant bias when applied directly to model the lake surface conditions. The reason was the difference in the physical characteristics, in particular, air temperatures and wind speeds, between land and water, which is especially strong over Tibet (Lazhu et al., 2016). The result is consistent with the findings of Kheyrollah Pour et al (2012), who applied the FLake model to Great Slave Lake and Big

Bear Lake in Canada. They also found that the model overestimated the LST compared with the MODIS data because the forcing data were obtained at the land station rather than over the lake surface. In our case, the ITPCAS air temperature was 0.71 °C larger during daytime and 2.49 °C smaller during nighttime compared to the buoy observations. The ITPCAS wind speeds were 0.63 $m \cdot s^{-1}$ lower during daytime and 1.83 $m \cdot s^{-1}$ lower during nighttime. In turn, the daily variations of the air temperature in ITPCAS data were almost 2.85 times higher than in the buoy observations. Lower wind speeds from ITPCAS forcing data weaken the heat transfer and leads to a warmer lake surface temperature simulated by FLake. Additionally, the wind speed of ITPCAS data is smaller at night corresponding with a higher simulated LST in the nighttime. This result proves that the deviation of the ITPCAS forcing data indeed leads to a warmer simulated LST. Hence, the choice of the atmospheric forcing is crucial for the simulation of large lakes in the extreme highland conditions of Tibet. In the absence of long-term weather observations over the lake surface, a correction procedure can be applied to the forcing data based on the available short-term observations from moored stations (buoys) and (or) satellite information. In this study, a comparison with a short-term observation data from the buoy on lake surface allowed correction of the ITPCAS forcing data significantly reducing the bias between the model and the remote sensing data.

Currently, there is no information available on the vertical thermal structure of Qinghai Lake. The stratification pattern simulated in this study is however very similar to the observations from other Tibetan lake, Bangong Co (Wang et al, 2014). Still, since the model used here is the freshwater lake model, the simulated mixing regime may have some difference with the actual situation of Qinghai Lake.

The good prediction of the LST over the Tibet by the relatively simple, highly parameterized model FLake, verified by satellite and buoy data, is one of the core results of this study. Both the importance of the Plateau for global climate interactions and the lack of continuous observations in this region demand reliable modeling schemes to take into account the complexity of the land-atmosphere interactions. FLake is currently among the few lake parameterization schemes actively used in regional climate models and numerical weather prediction (NWP). Complementary to the recent study of Kirillin et al. (2017), who successfully applied FLake to the freshwater lakes of TP, the present study demonstrates that the model adequately simulates the major mechanisms of the air-lake interaction in large brackish lakes of Tibet. Hence, FLake can significantly improve the simulation of the land-atmosphere interaction in regional climate models and NWP, which is crucial for understanding the climate-driven changes in this key region. To a first approximation, the result suggests the applicability of FLake to the simulation of all large brackish waters. The latter are characteristic features of arid regions worldwide having a strong impact on regional climate and water budget.

We have found that the duration of the ice-covered period is crucial for the lake-atmosphere interaction on the TP, with periods of ice-on and ice-off having the strongest effect both on the radiation balance and the boundary heat exchange by SH and LH. To simulate the ice cover duration properly, the heat storage in winter and the vertical heat transport across the ice-covered water column should be adequately described. In its present version, FLake treats these in a simplistic way, neglecting the heating of water column by solar radiation penetrating the ice cover (Kirillin et al., 2017). This simplification is a source of potential errors in the simulated ice break-up date and LST after the break-up, which errors can be significant for the Tibetan conditions, taking into account the strong solar radiation and low snow precipitation on TP in winter. In earlier studies on lowland lakes, FLake tended to predict earlier break-up dates because of the absence of snow in the FLake model (Bernhardt et al., 2012; Kheyrollah Pour et al., 2012). In this study, the simulated break-up date was generally later than observation, which can be treated as an indication of the importance of the under-ice water column heating by solar radiation neglected in the model. Another factor potentially introducing the uncertainty into the simulation of the ice duration is the ice albedo. The latter was recently estimated in Qinghai Lake to be much lower than typical estimates for lakes: ice albedo obtained by MODIS was less than 0.25 under the snow-free condition and less than 0.4 even under the snow cover condition (Li et al., 2018). Among the reasons for such a low ice albedo may be mentioned is the effects of salt on the ice structure and deformation of the ice surface under influence of the strong solar radiation. As a result, standard modeling approaches may underestimate the amount of shortwave radiation penetrating the ice, with subsequent errors predicting the ice duration and underestimation of the LST after ice break-up date.

The LST acquired by the MODIS, which was used as a reference for validation of simulation results, was generally lower than the in situ LST. This discrepancy was apparently contributed by the cool skin effect (Crosman and Horel, 2009), which is also found to be stronger in high-altitude lakes than in the ocean due to strong solar radiative heating and cooler air temperature at lake surface (Li et al., 2015; Wen et al., 2016). Keeping in mind the cool skin effect, we can suggest that the model predictions of the bulk LST are even better than the satellite data suggest, though exact estimation of the cool skin correction is out of the scope of this study.

### 4.2 Response of Qinghai Lake to climate change

As expected, the correlation analysis shows that the changes in LST were closely related to air temperatures and wind speed. The increase of the air temperature plays a key role in lake surface temperature warming, and the decrease in wind speed also promoted the warming of the lake surface temperature. Annual mean LST simulated by FLake increased at a rate of 0.66 °C per decade, primarily due to rising air temperature and decreasing wind speed. The warming trend of simulated LST significantly exceeded that of the regional air temperature (0.58 $°C \cdot decade^{-1}$). This discrepancy may be caused by declining winter ice cover, which leads to an earlier start of the stratified season that significantly increases the LST (Austin, 2007). Mixed-layer and water mean column temperature increasing 0.29 °C and 0.27 °C from 1979 to 2012 respectively, while the bottom temperature increased slowly from 1979 to 1989 and had even a slight decrease trend from 1989 to 2012. The slight decrease of the deep temperatures agrees with findings of Kirillin et al (2017) from freshwater Ngoring Lake in TP, and the research of Huang et al. (2017) that use the GLM lake model at another TP lake Nam Co. The apparent reason for the deep cooling is the increase of stability of the lake due to surface warming, which restricts heat transfer from surface to bottom and produces a decrease of the bottom water temperature. This behavior has been reported as a characteristic in previous studies on lowland dimictic lakes (Hondzo and Stefan,1993; Danis et al.,2004; Kirillin, 2010).

The simulated seasonal stratification regime suggests Qinghai Lake be dimictic, with the spring overturn taking place around May and the autumn overturn appearing around November-December, given the effect of salinity on stratification is of secondary importance compared with temperature. While salinity effects require further investigation, the modeled mixing regime may be suggested to be close to the reality, taking into account the low salt content and strong seasonal variations in lake temperatures.

As mentioned above, climate change was found to have a strong impact on the lake ice phenology. The maximum ice thickness of Qinghai Lake was decreasing in simulations, significant tendencies to later ice-on and earlier ice-off were predicted. These three ice phenology characteristics were correlated with the January-April, November-December, and March-April air temperature respectively. The ability to accurately represent ice cover on lakes is essential for the improvement of global circulation models, regional climate models and numerical weather forecasting (Brown, 2010). We have shown that the net shortwave radiation increase caused by shortening of the ice duration plays a key role in net radiation increase. So, we argue that the declining winter ice cover has a much significant influence on annual radiation balance of the lake.

In total, the annual energy storage by Qinghai Lake (the total annual heat input Q) decreased at a slow rate of -0.31 $W \cdot m^{-2}$ per decade, balanced primarily by the increase of received net radiation and released latent heat flux at the surface (Fig. 8 e). Still, the average value of Q in the simulation period remained positive, i.e. lake was continuously warming with the accumulated energy stored by the lake increasing at 4.17 $W \cdot m^{-2}$ per decade ($p>0.01$) (Fig. 8 f), consistent with the trend of the mean water column temperature. The change of freeze-up/break-up date dramatically influenced the lake energy and heat budget during the ice formation/decay period. The earlier thaw of ice caused an increase of energy absorbed by the lake in late spring since more solar radiation was absorbed by the lake without reflection by the ice cover. The delayed freeze-up date lead to an increase in energy lost before freeze-up due to strong upward longwave radiation, SH and LH.

### 4.3 Differences between the highland TP lakes and lakes of other regions

For low-altitude lakes in other regions, the air temperature is typically higher than LST between the ice melt and the temperature equilibration in the mid-summer. In the later surface cooling in autumn, the LST remain higher than the air temperature down to the ice on. The seasonal pattern remains valid for both large (Rouse et al., 2003) and small (Nordbo et al., 2011) lakes. Due to a higher altitude, the lakes on the TP have a lower atmospheric thickness and air density, the solar radiation over the plateau is much stronger than in other areas of the same latitude, while the air temperatures are comparably low. These unique climatic conditions cause a significantly different seasonal interaction between the lake and the atmosphere (Wen et al., 2016). In this study, the LST of Qinghai lake increased very fast after ice melt in mid-April under the strong solar radiation and equilibrated with air temperature in June, which is much earlier than low-altitude lakes. The difference between air temperature and LST is the fundamental property of lake-air interaction, determining the intensity of the surface heat exchange by means of atmospheric stability. When the LST is higher than air temperature, which is the case of TP lakes in summer, the atmosphere over the lake becomes increasingly unstable, accelerating the release of heat to the atmosphere by convection. In that sense, the role of lakes, as hot-spots of the land-atmosphere interaction on the TP, consists in the accumulation of the solar radiation and release of the accumulated heat into the air by the convective exchange. This fact explains also the differences in the response of TP lakes to regional climate change compared to that found previously in low-altitude areas.

## Data availability

ITPCAS dataset is available in the Third Pole Environment Database (http://en.tpedatabase.cn/portal/). The lake model FLake is available from the model community site (http://www.lake model.net). The model configuration files and the output of the lake model are available from the first author by request.

## Author contribution

D. Su and L. Wen conceived the study. X. Hu provided the buoy data. D. Su performed the modeling with contributions from L. Wen and G. Kirillin. L. Zhao, Z. Li and J. Du performed analysis of remote sensing data. D. Su, L. Wen, and G. Kirillin analyzed the model output. D. Su wrote the paper with contributions from all co-authors.

## Competing interests

The authors declare that they have no conflict of interest.

## Acknowledgements

The study was supported by the National Natural Science Foundation of China (91637107, 41475011, 41811530387). The study is a part of the bilateral research project GZ1259 supported by the Sino-German Center for Research Support. G. Kirillin was supported by the German Science Foundation (DFG Projects KI-853-7/1, KI-853-11/1). Authors are grateful to M. Leppäranta for advice and comments on the paper.

## References

Austin, J. A., and Colman, S. M.: Lake Superior summer water temperatures are increasing more rapidly than regional air temperatures: A positive ice-albedo feedback, J. Geophys. Res. Lett., 34, L06604, doi:10.1029/2006GL029021, 2007.

Adrian, R., O'Reilly, C. M., Zagarese, H., Baines S. B., Hessen, D. O., Keller, W., Livingstone, D. M., Sommaruga, R., Straile, D., Van, D. E., Weyhenmeyer, G. A., Winder, M.: Lakes as sentinels of climate change, J. Limnol. Oceanogr., 54, doi:10.4319/lo.2009.54.6_part_2.2283, 2009.

Bonan, G. B.: Sensitivity of a GCM Simulation to Inclusion of Inland Water Surfaces, J. Climate, 8, 2691–2704, doi:10.1175/1520-0442(1995)008<2691:SOAGST>2.0.CO;2,1995.

Boehrer, B., and Schultze, M.: Stratification of lakes, Rev. Geophys., 46, RG2005, doi:10.1029/2006RG000210, 2008.

Brown, L. C. and Duguay, C. R.: The response and role of ice cover in lake-climate interactions, Prog. Phys. Geog.: Earth and Environment, 34, 671-704, doi:10.1177/0309133310375653, 2010.

Bernhardt, J., Engelhardt, C., Kirillin, G., Matschullat, J.: Lake ice phenology in Berlin-Brandenburg from 1947-2007: observations and model hindcasts, Clim. Change, 112, 791–817, 2012.

Crawford, T. M. and Duchon, C. E.: An improved parameterization for estimating effective atmospheric emissivity for use in calculating daytime downwelling longwave radiation, J. Appl. Meteorol., 38, 474–480, doi:10.1175/1520-0450(1999)038<0474:AIPFEE>2.0.CO;2, 1999.

Crosman, E. T. and Horel, J. D.: MODIS-derived surface temperature of the Great Salt Lake, Remote Sens. Environ., 113, 73–81, doi:10.1016/j.rse.2008.08.013, 2009.

Chen, Y., Yang, K., He, J., Qin, J., Shi, J., Du, J., and He, Q.: Improving land surface temperature modeling for dry land of China, J. Geophys. Res., 116, D20104, doi:10.1029/2011JD015921, 2011.

Cui, B. L. and Li, X. Y.: The impact of climate changes on water level of Qinghai Lake in China over the past 50 years, Hydrol. Res., 47, 532–542, doi:10.2166/nh.2015.237, 2015.

Donlon, C. J., Minnett, P. J., Gentemann, C., Nightingale, T. J., Barton, I. J., Ward, B., and Murray, M. J.: Toward Improved Validation of Satellite Sea Surface Skin Temperature Measurements for Climate Research, J. Climate, 15, 353–369, doi:10.1175/1520-0442(2002)015<0353:TIVOSS>2.0.CO;2, 2002.

Danis, P. A., Grafenstein, U. V., Masson-Delmotte, V., Planton, S., Gerdeaux, D., and Moisselin, J. M.: Vulnerability of two European lakes in response to future climatic changes, Geophys. Res. Lett., 31, L21507, doi:10.1029/2004GL020833, 2004.

Duan, A. M. and Wu, G. X.: Role of the Tibetan Plateau thermal forcing in the summer climate patterns over subtropical Asia, Clim. Dyn., 24, 793–807, doi:10.1007/s00382-004-0488-8, 2005.

Duan, A. and Xiao, Z.: Does the climate warming hiatus exist over the Tibetan Plateau?, Sci. Rep., 5, 13711, doi:10.1038/srep13711, 2015

Duguay, C. R., Prowse, T. D., Bonsal, B. R., Brown, R. D., Lacroix, M. P., and Ménard, P.: Recent trends in Canadian lake ice cover, Hydrol. Process., 20, 781–801, doi:10.1002/hyp.6131, 2006.

Desai, A. R., Austin, J. A., Bennington, V., and McKinley, G. A.: Stronger winds over a large lake in response to weakening air-to-lake temperature gradient, Nat. Geosci., 2, 855–858, doi:10.1038/ngeo693, 2009.

Dutra, E., Stepanenko, V. M., Balsamo, G., Viterbo, P., Miranda, P. M. A., Mironov, D., and Schär, C.: An offline study of the impact of lakes on the performance of the ECMWF surface scheme, Boreal Environ. Res., 15, 100–112, 2010.

Deng, S., Dong, H., Lv, G., Jiang, H., Yu, B., and Bishop, M. E.: Microbial dolomite precipitation using sulfate reducing and halophilic bacteria: Results from Qinghai Lake, Tibetan Plateau, NW China, Chem. Geol., 278, 151–159, doi:10.1016/j.chemgeo.2010.09.008, 2010.

Dong, H. and Song, Y.: Shrinkage history of Lake Qinghai and causes during the last 52 years, 2011 International Symposium on Water Resource and Environmental Protection (ISWREP), Xi'an, China, 20-22 May 2011, 446–449, 2011.

Ding, Z., Lu, R., Liu, C., and Duan, C.: Temporal change characteristics of climatic and its relationships with atmospheric circulation patterns in Qinghai Lake Basin, Advances in Earth Science (in Chinese), 33, 281–292, doi:10.11867/j.issn.1001-8166.2018.03.0281, 2018.

Eerola, K., Rontu, L., Kourzeneva, E., and Shcherbak, E.: A study on effects of lake temperature and ice cover in HIRLAM, Boreal. Environ. Res., 15,130–142, 2010.

Gao, Y., Tang, M., Luo, S., Shen, Z., and Li, C.: Some aspects of recent research on the Qinghai-Xizang Plateau meteorology, Bull. Am. Meteorol. Soc., 62, 31–35, doi:10.1175/1520-0477(1981)062<0031:SAORRO>2.0.CO;2, 1981.

Guo, D. and Wang, H.: The significant climate warming in the northern Tibetan Plateau and its possible causes, Int. J. Climatol., 32, 1775–1781, doi:10.1002/joc.2388, 2012.

Guo, D. and Wang, H.: Simulation of permafrost and seasonally frozen ground conditions on the Tibetan Plateau, 1981–2010, J. Geophys. Res. Atmos., 118, 5216–5230, doi:10.1002/jgrd.50457, 2013.

He, J.: Development of a Surface Meteorological Dataset of China with High Temporal and Spatial Resolution, Ph.D. thesis, Institute of Tibetan Plateau Research, Chinese Academy of Science, China, 2010.

He, J. and Yang, K.: China meteorological forcing dataset, Cold and Arid Regions Science Data Center at Lanzhou, 2011.

Hondzo, M. and Stefan, H. G.: Regional water temperature characteristics of lakes subjected to climate change, Clim. Change, 24,187–211, doi:10.1007/BF01091829, 1993.

Huang, L., Wang, J., Zhu, L., Ju, J., and Daut, G.: The warming of large lakes on the Tibetan Plateau: Evidence from a lake model simulation of Nam Co, China, during 1979–2012, J. Geophys. Res. Atmos., 122, 13095–13107, doi:10.1002/2017JD027379, 2017.

Haginoya, S., Fujii, H., Kuwagata, T., Xu, J., Ishigooka, Y., Kang, S., and Zhang, Y.: Air-lake interaction features found in heat and water exchanges over Nam Co on the Tibetan Plateau, Sola, 5, 172–175, doi:10.2151/sola.2009-044, 2009

Jakkila, J., Leppäranta, M., Kawamura, T., Shirasawa, K., and Salonen, K.: Radiation transfer and heat budget during the ice season in Lake Pääjärvi, Finland, Aquat. Ecol., 43, 681–692, doi:10.1007/s10452-009-9275-2, 2009.

Kirillin, G.: Modeling the impact of global warming on water temperature and seasonal mixing regimes in small temperate lakes, Boreal Environ. Res., 15, 279–293, 2010.

Kirillin, G. and Shatwell, T.: Generalized scaling of seasonal thermal stratification in lakes, Earth-Sci. Rev., 161, 179–190, doi:10.1016/j.earscirev.2016.08.008, 2016.

Kirillin, G., Wen, L., and Shatwell, T.: Seasonal thermal regime and climatic trends in lakes of the Tibetan highlands, Hydrol. Earth Syst. Sci., 21, 1895–1909, doi:10.5194/hess-21-1895-2017, 2017.

Kheyrollah Pour, H., Duguay, C. R., Martynov, A., and Brown, L. C.: Simulation of surface temperature and ice cover of large northern lakes with 1-D models: a comparison with MODIS satellite data and in situ measurements, Tellus A: Dynamic Meteorology and Oceanography, 64, 17614, doi:10.3402/tellusa.v64i0.17614, 2012.

Kitaigorodskii, S. A. and Miropolsky, Y. Z.: On theory of open ocean active layer, Izvestiya Akademii Nauk SSSR Fizika Atmosfery I Okeana, 6, 177–188, 1970.

Livingstone, D. M.: Impact of secular climate change on the thermal structure of a large temperate central European lake, Clim. Change, 57, 205–225, doi:10.1023/A:1022119503144, 2003.

Livingstone, D. M.: A Change of Climate Provokes a Change of Paradigm: Taking Leave of Two Tacit Assumptions about Physical Lake Forcing, Int. Rev. Hydrobiol., 93, 404–414, doi:10.1002/iroh.200811061, 2008.

Latifovic, R., Pouliot, D.: Analysis of climate change impacts on lake ice phenology in Canada using the historical satellite data record, Remote. Sens. Environ., 106, 492–507, doi:10.1016/j.rse.2006.09.015, 2007.

Leppäranta, M., Lewis, J. E.: Observations of ice surface temperature and thickness in the Baltic Sea, Int. J. Remote Sens., 28, 3963–3977, doi:10.1080/01431160601075616, 2007.

Li, X. Y., Xu, H. Y., Sun, Y. L., Zhang, D. S., and Yang, Z. P.: Lake-Level Change and Water Balance Analysis at Lake Qinghai, West China during Recent Decades, Water Resour. Manag., 21, 1505–1516, doi:10.1007/s11269-006-9096-1, 2007.

Li, X. Y., Ma, Y. J., Huang, Y. M., Hu, X., Wu, X. C., Wang, P., Li, G. Y., Zhang, S. Y., Wu, H. W., Jiang, Z. Y., Cui, B. L., and Liu, L.: Evaporation and surface energy budget over the largest high-altitude saline lake on the Qinghai-Tibet Plateau, J. Geophys. Res. Atmos., 121, 10470–10485, doi:10.1002/2016JD025027, 2016.

Langer, M., Westermann, S., Boike, J.: Spatial and temporal variations of summer surface temperatures of wet polygonal tundra in Siberia-implications for MODIS LST based permafrost monitoring, Remote Sens. Environ., 114, 2059–2069, doi:10.1016/j.rse.2010.04.012, 2010.

Liu, J. G. and Xie, Z. H.: Improving simulation of soil moisture in China using a multiple meteorological forcing ensemble approach, Hydrol. Earth Syst. Sci., 17, 3355–3369, doi:10.5194/hess-17-3355-2013, 2013.

Liao, J., Shen, G., and Li, Y.: Lake variations in response to climate change in the Tibetan Plateau in the past 40 years, Int. J. Digit. Earth, 6, 534–549, doi:10.1080/17538947.2012.656290, 2013.

Lei, Y., Yang, K., Wang, B., Shen, Y., Bird, B. W., Zhang, G., and Tian, L.: Response of inland lake dynamics over the Tibetan Plateau to climate change, Clim. Change, 125, 281–290, doi:10.1007/s10584-014-1175-3, 2014.

Li, Z., Lyu, S., Ao, Y., Wen, L., Zhao, L., and Wang, S.: Long-term energy flux and radiation balance observations over Lake Ngoring, Tibetan Plateau, Atmos. Res., 155, 13–25, doi:10.1016/j.atmosres.2014.11.019, 2015.

Li, Z., Ao, Y., Lyu, S., Lang, J.: Investigation of the ice surface albedo in the Tibetan Plateau lakes based on the field observation and MODIS products, J. Glaciol., 64, 506–516, doi:10.1017/jog.2018.35, 2018.

Lazhu, Yang, K., Wang, J., Lei, Y., Chen, Y., Zhu, L., Ding, B., and Qin, J.: Quantifying evaporation and its decadal change for Lake Nam Co, central Tibetan Plateau, J. Geophys. Res. Atmos., 121, 7578–7591, doi:10.1002/2015JD024523, 2016.

Minnett, P. J.: Radiometric measurements of the sea-surface skin temperature: The competing roles of the diurnal thermocline and the cool skin, Int. J. Remote. Sens., 24, 5033–5047, doi:10.1080/0143116031000095880, 2003.

Mironov, D.V.: Parameterization of lakes in numerical weather prediction. Description of a lake model. COSMO Technical Report, Deutscher Wetterdienst, Offenbach am Main, Germany, 2008.

Ma, R. H., Yang, G. S., Duan, H. T., Jiang, J. H., Wang, S. M., Feng, X. Z., Li, A. N., Kong, F. X., Xue, B., Wu, J. L., and Li, S. J.: China's lakes at present: number, area and spatial distribution, Sci. China Earth Sci., 54, 283–289, doi:10.1007/s11430-010-4052-6, 2011.

Ma, Y., Wang, Y., Wu, R., Hu, Z., Yang, K., Li, M., Ma, W., Zhong, L., Sun, F., Chen, X., Zhu, Z., Wang, S., and Ishikawa, H.: Recent advances on the study of atmosphere-land interaction observations on the Tibetan Plateau, Hydrol. Earth Syst. Sci., 13, 1103–1111, doi:10.5194/hess-13-1103-2009, 2009.

Magnuson, J. J., Robertson, D. M., Benson, B. J., Wynne, R. H., Livingstone, D. M., Arai, T., Assel, R. A., Barry, R. G., Card, V., Kuusisto, E., Granin, N. G., Prowse, T. D., Stewart, K. M., and Vuglinski, V. S.: Historical trends in lake and river ice cover in the Northern Hemisphere, Science, 289, 1743–1746, doi:10.1126/science.289.5485.1743, 2000.

Mallard, M. S., Nolte, C. G., Bullock, O. R., Spero, T. L., and Gula, J.: Using a coupled lake model with WRF for dynamical downscaling, J. Geophys. Res. Atmos., 119, 7193–7208, doi: 10.1002/2014JD021785, 2014.

Nordbo, A., Launiainen, S., Mammarella, I., Leppäranta, M., Huotari, J., Ojala, A., and Vesala, T.: Long-term energy flux measurements and energy balance over a small boreal lake using eddy covariance technique, J. Geophys. Res., 116, D02119, doi:10.1029/2010JD014542, 2011.

O'Reilly, C. M., Sharma, S., Gray, D. K., Hampton, S. E., Read, J. S., Rowley, R. J., Schneider, P., Lenters, J. D., McIntyre, P. B., Kraemer, B. M., et al., Rapid and highly variable warming of lake surface waters around the globe, Geophys. Res. Lett., 42,10773–10781, doi:10.1002/2015GL066235, 2015.

Qiu, J.: China: The third pole, Nature, 454, 393–396, doi:10.1038/454393a, 2008.

Robinson, I. S., Wells, N. C., Charnock, H.: The sea surface thermal boundary layer and its relevance to the measurement of sea surface temperature by airborne and spaceborne radiometers, Int. J. Remote Sens., 5, 19–45, doi:10.1080/01431168408948787, 1984.

Rouse, W. R., Oswald, C. M., Binyamin, J., Blanken, P. D., Schertzer, W. M., and Spence, C.: Interannual and seasonal variability of the surface energy balance and temperature of central Great Slave Lake, J. Hydrometeorol., 4, 720–730, doi:10.1175/1525-7541(2003)004<0720:IASVOT>2.0.CO;2, 2003.

Rooney, G. G., Bornemann, F. J.: The performance of FLake in the Met Office Unified Model, Tellus, 65, 1089–1108, doi:10.3402/tellusa.v65i0.21363, 2013.

Salgado, R., Le Moigne, P.: Coupling of the FLake model to the Surfex externalized surface model, Boreal Environ. Res., 15, 231–244, 2010.

Stepanenko, V. M., Martynov, A., Johnk, K. D., Subin, Z. M., Perroud, M., Fang, X., Beyrich, F., Mironov, D., and Goyette, S.: A one-dimensional model intercomparison study of thermal regime of a shallow, turbid midlatitude lake, Geosci. Model Dev., 6, 1337–1352, doi:10.5194/gmd-6-1337-2013, 2013.

Schmid, M., Hunziker, S., Wüest, A.: Lake surface temperatures in a changing climate: A global sensitivity analysis, Clim. Change, 124, 301–315, doi:10.1007/s10584-014-1087-2, 2014.

Shen, M., Piao, S., Jeong, S.-J., Zhou, L., Zeng, Z., Ciais, P., Chen, D., Huang, M., Jin, C.-S., Li, L. Z. X., Li, Y., Myneni, R. B., Yang, K., Zhang, G., Zhang, Y., and Yao, T.: Evaporative cooling over the Tibetan Plateau induced by vegetation growth, P. Nat. Acad. Sci. USA, 112, 9299–9304, doi:10.1073/pnas.1504418112, 2015.

Thiery, W., Martynov, A., Darchambeau, F., Descy, J.P., Plisnier, P.D., Sushama, L., van Lipzig, N.P.M.: Understanding the performance of the FLake model over two African Great Lakes. Geosci. Model Dev., 7, 317–337, doi:10.5194/gmd-7-317-2014, 2014.

Tang, L., Duan, X., Kong, F., Zhang, F., Zheng, Y., Li, Z., Mei, Y., Zhao, Y., and Hu, S.: Influences of climate change on area variation of Qinghai Lake on Qinghai-Tibetan Plateau since 1980s, Sci. Rep., 8, 7331, doi:10.1038/s41598-018-25683-3, 2018.

Wan, Z., Zhang, Y., Zhang, Q., and Li, Z. L.: Quality assessment and validation of the MODIS global land surface temperature, Int. J. Remote. Sens., 25, 261–274, doi:10.1080/0143116031000116417, 2004.

Weyhenmeyer, G. A., Meili, M., Livingstone, D. M.: Nonlinear temperature response of lake ice breakup[J]. Geophys. Res. Lett., 31, doi:10.1029/2004GL019530, 2004.

Williamson C. E., Saros J. E., Vincent W. F., Smol J. P.: Lakes and reservoirs as sentinels, integrators, and regulators of climate change, Limnol. Oceanogr., 54, 2273–2282, doi:10.4319/lo.2009.54.6_part_2.2273, 2009.

Wang, M., Hou, J., Lei, Y.: Classification of Tibetan lakes based on variations in seasonal lake water temperature, Chin. Sci. Bull., 59, 4847–4855, doi:10.1007/s11434-014-0588-8, 2014.

Wen, L., Lyu, S., Kirillin, G., Li, Z., and Zhao, L.: Air–lake boundary layer and performance of a simple lake parameterization scheme over the Tibetan highlands, Tellus A, 68, 31091, doi:10.3402/tellusa.v68.31091, 2016.

Xu, X., Lu, C., Shi, X., and Gao, S.: World water tower: An atmospheric perspective, Geophys. Res. Lett., 35, 525–530, doi:10.1029/2008GL035867, 2008.

Yanai, M., Li, C., Song, Z.: Seasonal heating of the Tibetan Plateau and its effects on the evolution of the Asian summer monsoon, Journal of the Meteorological Society of Japan, 70, 319–351, doi:10.2151/jmsj1965.70.1B_319, 1992.

Ye, Q., Wei, Q., Hochschild, V., and Duguay, C. R.: Integrated observations of lake ice at Nam Co on the Tibetan Plateau from 2001 to 2009, 2011 IEEE International Geoscience and Remote Sensing Symposium (IGARSS), Vancouver, BC, Canada, 24-29 July 2011, 3217–3220, 2011.

Yang, K., Wu, H., Qin, J., Lin, C., Tang, W., and Chen Y.: Recent climate changes over the Tibetan Plateau and their impacts on energy and water cycle: A review, Glob. Planet. Change, 112, 79–91, doi:10.1016/j.gloplacha.2013.12.001, 2014.

Yao, X., Li, L., Zhao, J., Sun, M., Li, J., Gong, P., and An, L.: Spatial-temporal variations of lake ice phenology in the Hoh Xil region from 2000 to 2011, J. Geogr. Sci., 26, 70–82, doi:10.1007/s11442-016-1255-6, 2016.

Zhang, G., Xie, H., Kang, S., Yi, D., and Ackley, S. F.: Monitoring lake level changes on the Tibetan Plateau using ICESat altimetry data (2003–2009), Remote. Sens. Environ., 115, 1733–1742, doi:10.1016/j.rse.2011.03.005, 2011.

Zhang, G., Yao, T., Xie, H., Qin, J., Ye Q., Dai, Y., and Guo, R.: Estimating surface temperature changes of lakes in the Tibetan Plateau using MODIS LST data, J. Geophys. Res. Atmos., 119, 8552–8567, doi:10.1002/2014JD021615, 2014a.

Zhang, G., Yao, T., Xie, H., Zhang, K., and Zhu, F.: Lakes' state and abundance across the Tibetan Plateau, Sci. Bull. (Beijing), 59, 3010–3021, doi:10.1007/s11434-014-0258-x, 2014b.

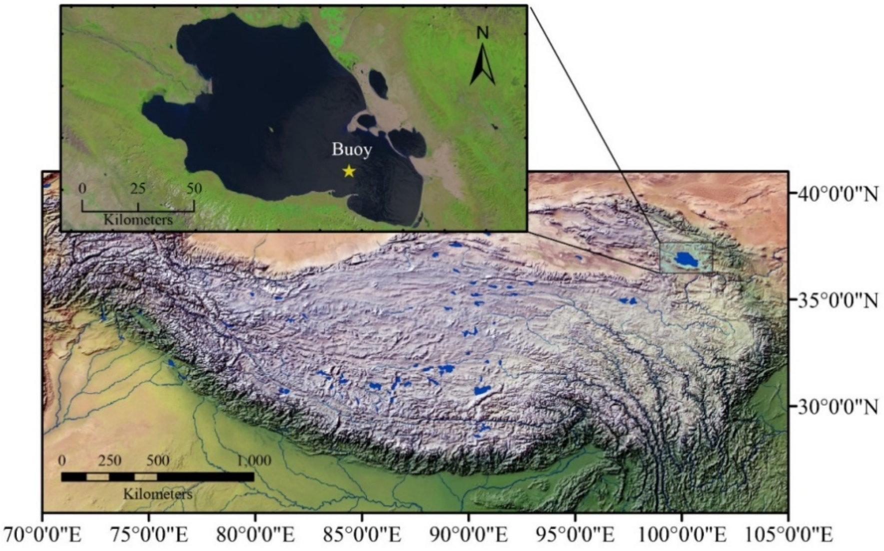

**Figure 1: Study area and the location of buoy station.**

Hydrol. Earth Syst. Sci. Discuss., https://doi.org/10.5194/hess-2018-583
Manuscript under review for journal Hydrol. Earth Syst. Sci.
Discussion started: 13 December 2018

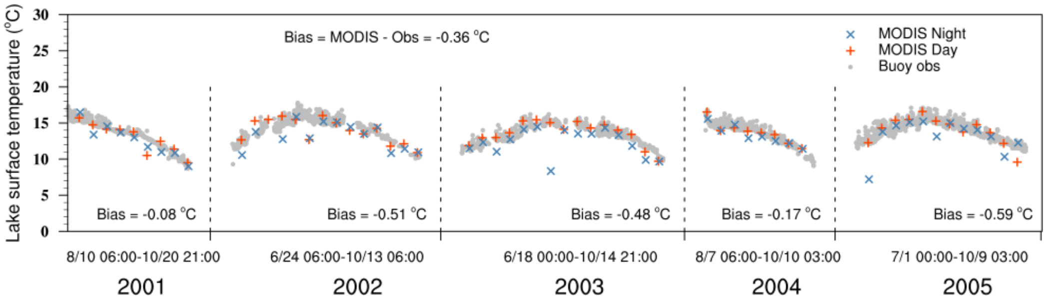

**Figure 2: Comparison of the lake surface temperature between observations by buoy and MODIS respectively.**

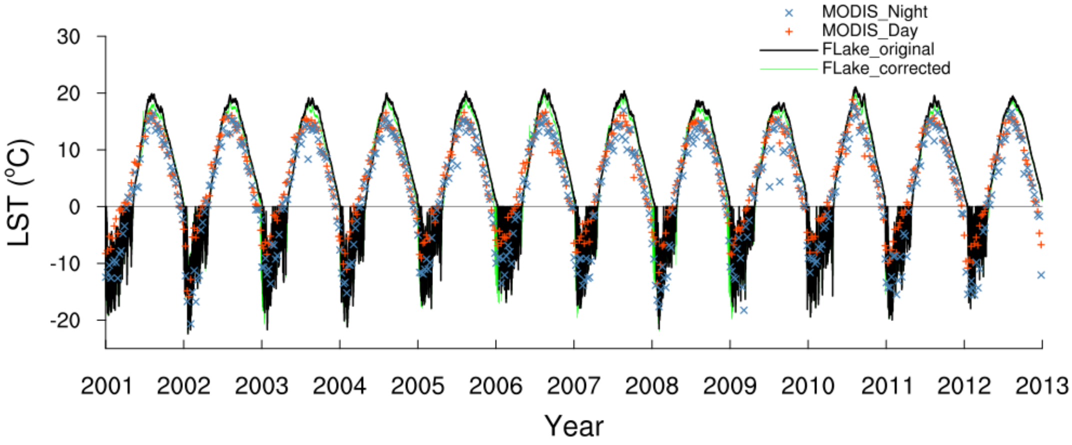

**Figure 3: Comparison of lake surface temperature between FLake simulation forced by original (thick line) and corrected (thin line) ITPCAS data and MODIS observation (symbols).**

5

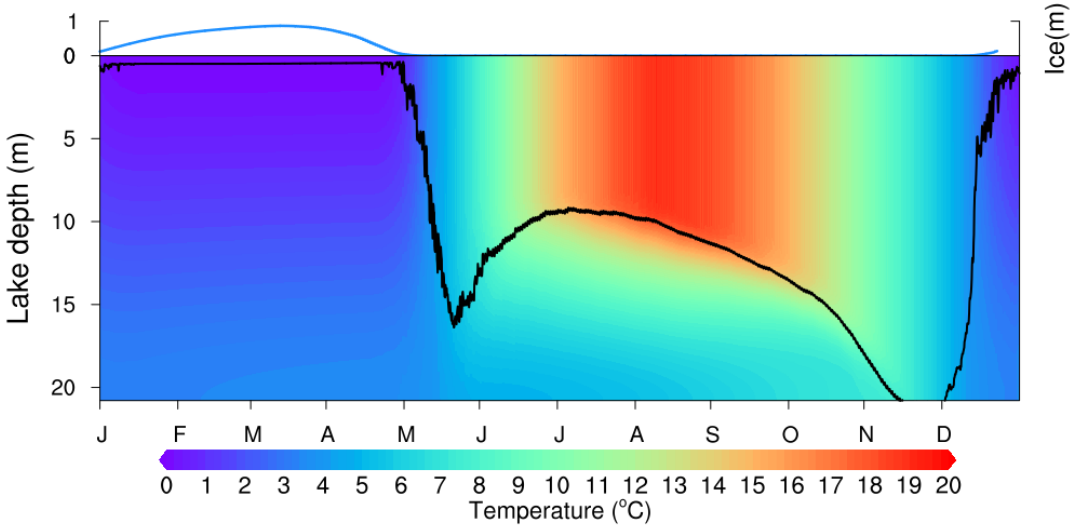

**Figure 4: The modeled seasonal thermal stratification pattern and ice cover of Qinghai Lake averaged from 1979 to 2012. The blue line is ice cover thickness and the black one is the depth of mixed layer.**

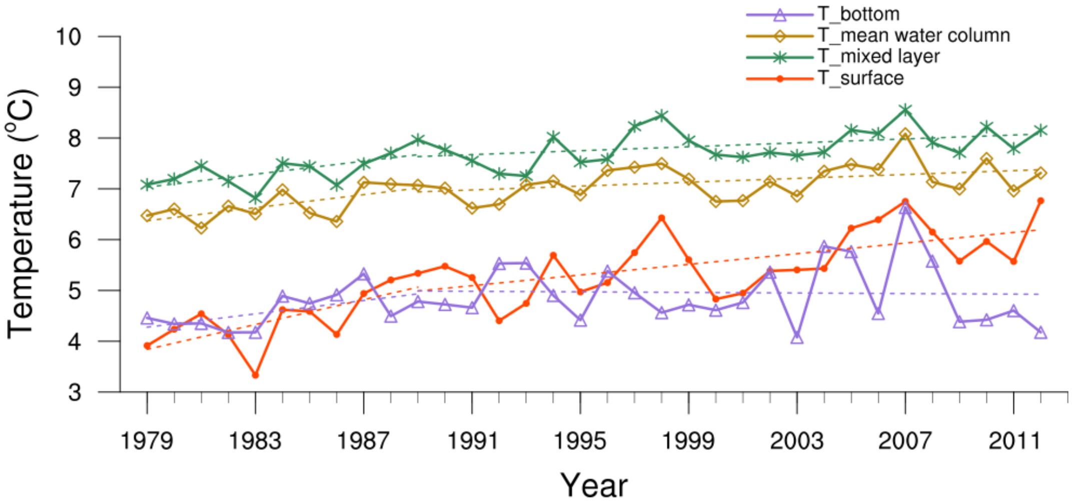

**Figure 5: Annual variation trends of the lake water temperature at the surface, mixed-layer, mean water column and bottom layer respectively.**

5

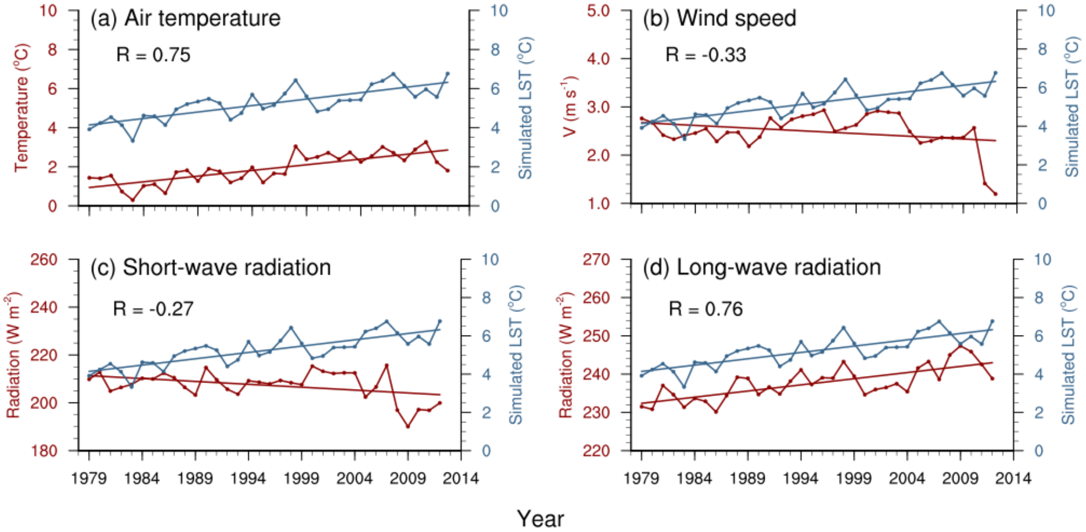

**Figure 6: Interannual variations in air temperature (a), wind speed (b), short-wave radiation(c) and long-wave radiation (d) for Qinghai Lake and their correlations to simulated annual mean lake surface temperature (LST) from 1979 to 2012.**

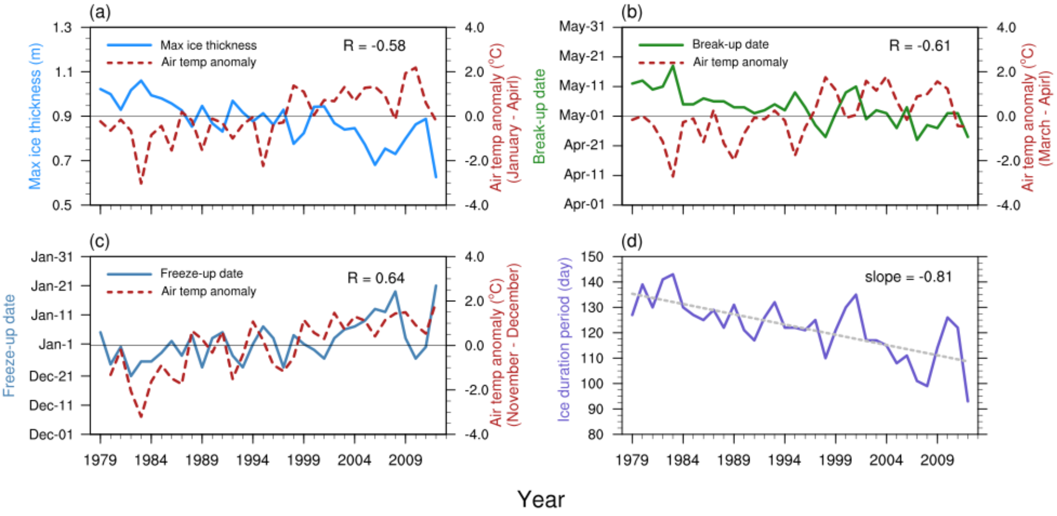

**Figure 7: The interannual variations of maximum annual ice thickness (a), break-up date (b), freeze-up date (c) and ice duration period (d) of Qinghai Lake. The red dash line is air temperature anomaly in the specified period.**

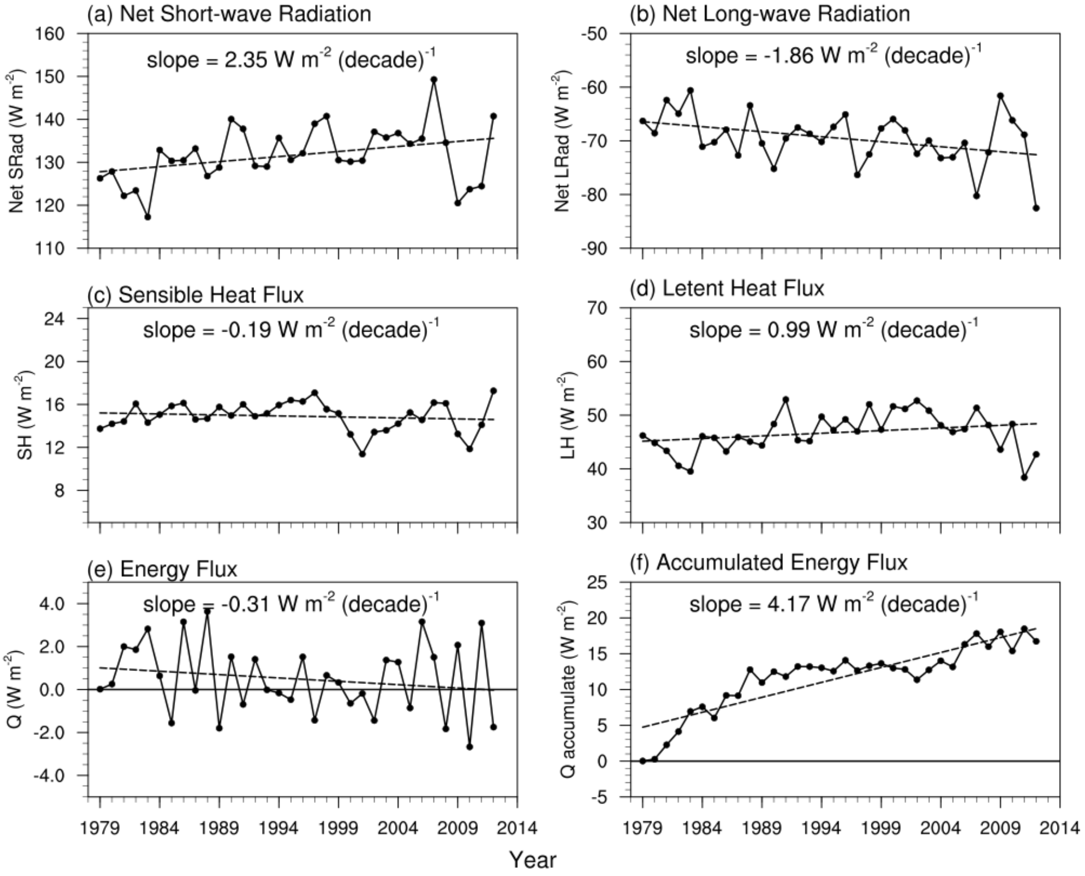

**Figure 8: The interannual variation trend of simulated annual mean lake surface net shortwave radiation (a), net longwave radiation(b), sensible heat flux(c), latent heat flux (d), net energy flux (e) and cumulative net energy flux (f) from 1979 to 2012.**

5

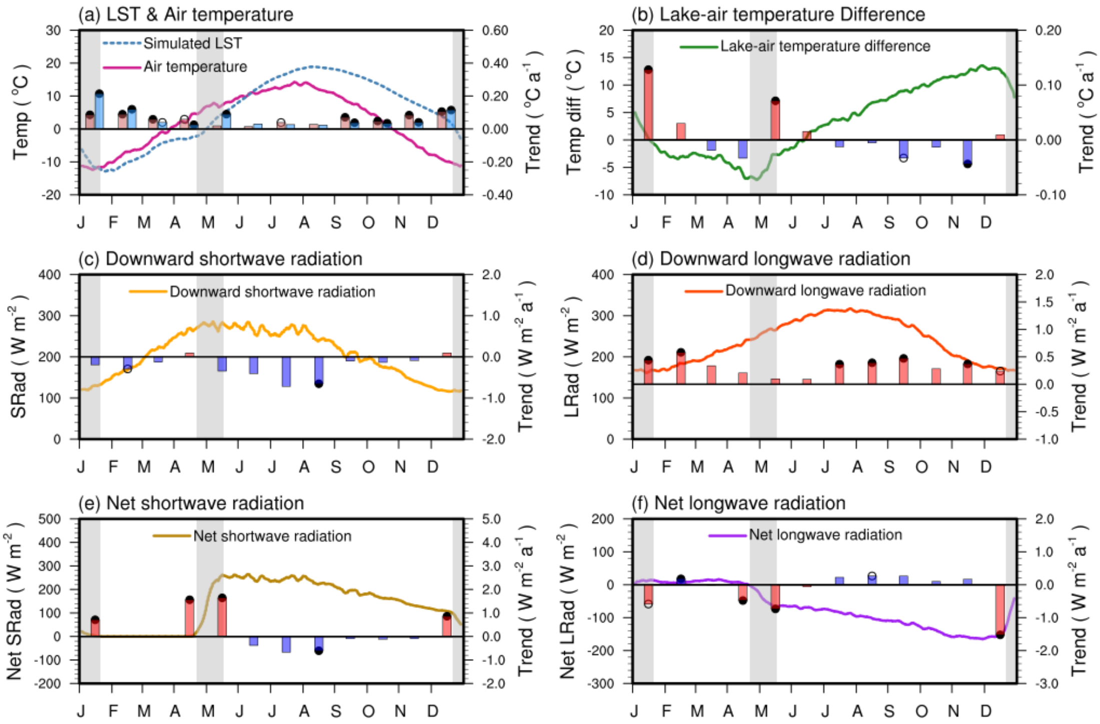

**Figure 9: Climatological mean seasonal variations (5-day moving average, lines) in simulated LST and air temperature (a) with their difference (b), downward shortwave radiation(c), downward longwave radiation(d), net shortwave radiation (e) and net longwave radiation (f). The bars indicate monthly averaged mean annual variation trend (red for positive and blue for negative) from 1979 to 2012. Solid points at end of the bars mean pass significance test of $p<0.01$ and hollow points mean $p<0.05$. The grey areas indicate the freeze-up and break-up date variation range of the lake.**

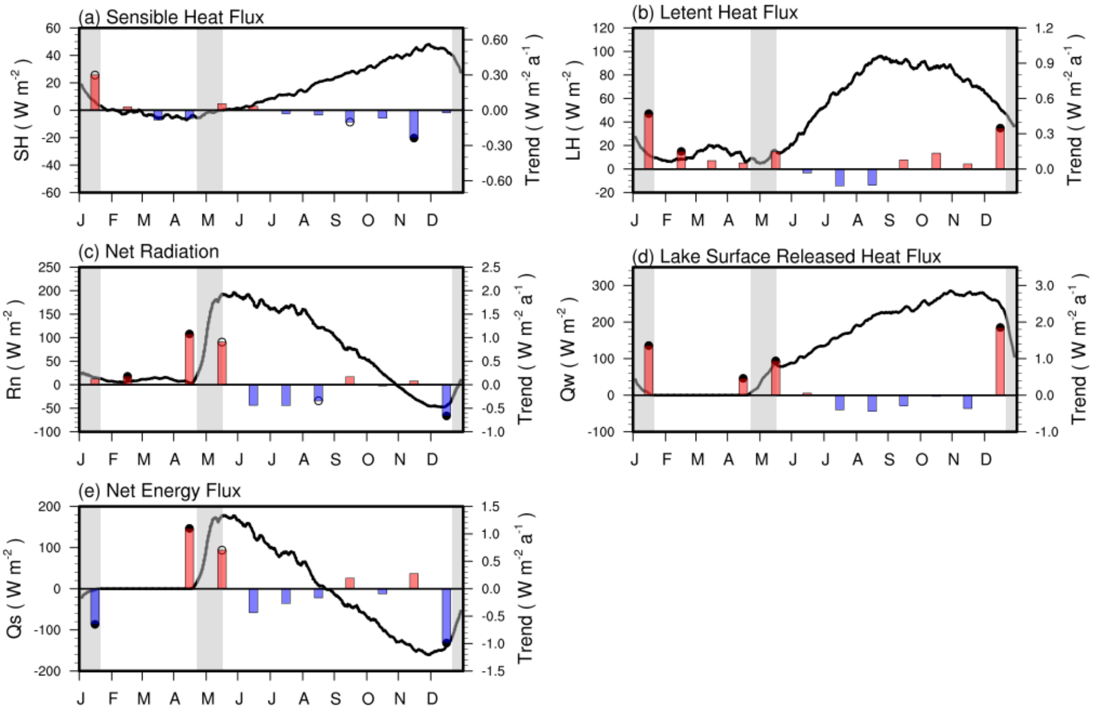

**Figure 10: Climatological mean seasonal variations (5-day moving average, lines) in the simulated sensible heat flux (a), latent heat flux (b), net radiation (c), lake surface released heat flux (d) and net energy flux (e). The bars indicate their monthly averaged mean annual variation trend (red for positive and blue for negative) from 1979–2012. Solid points at end of the bars mean pass significance test of p<0.01 and hollow points mean p<0.05. The grey areas indicate the freeze-up and break-up date variation range of the lake.**